Supplementary Information

1. Silica rod synthesis and characterization

Materials: Acetone (99.99 %, LachNer), 1-pentanol (98 %, Alfa Aesar), ethanol (98 %, Aldrich), polyvinylpyrrolidone 40 k (PVP, Aldrich), ammonium hydroxide solution (25 wt%, Aldrich), sodium citrate dihydrate (99.0 %, Aldrich), tetraethyl orthosilicate (TEOS, 98 %, Aldrich) and fluorescein isothiocyanate (FITC, > 90 %, Aldrich) were used as received. Milli-Q water (18.2 MΩ.cm, Millipore Inc.) was used for all experiments.

Silica rods were obtained via a "large batch" synthesis. Typically, 120 g polyvinylpyrrolidone were dissolved in 1.2 L of 1-pentanol by sonication in a water bath for 4 h to prepare the polymer solution. Next, 32.4 mL Milli-Q water, 7.2 mL sodium citrate solution (0.18 M) and 128 mL ethanol were added to the polymer solution. The mixture was stirred with an overhead stirrer for 5 min, before the addition of 24.3 mL ammonium hydroxide solution and 10.8 mL TEOS, followed by stirring for 30 sec. After 4 h, 5.4 mL TEOS were added and the flask was gently shaken by hand. The reaction was stopped after 15 h and the reaction medium was centrifuged at 4400×G for 1.5 h. The rods were recovered, washed, and size separated by successive centrifugation and re-dispersion cycles (4 times in ethanol at 736×G for 12 min, 4 times in water at 736×G for 12 min and 8 times in water at 304×G for 12 min). The precipitate was retained and the smaller rods in the supernatant were removed. Afterwards, very large rods were removed by two centrifugation cycles in water at 60×G, the supernatant was retained and the precipitate was discarded.

The size distribution of the synthesized rods (Figure S1) was determined by field emission scanning electron microscopy (FE-SEM, JEOL JSM-7000F) using an image processing software (ImageJ). A minimum of 200 rods were analyzed to determine the distribution in the measured particle dimensions. The silica rods synthesized had an average length of 4.36 μm with a length polydispersity of 18 % and an average aspect ratio of 10.

The silica rod density was measured using an oscillating U – tube density meter (DMA 4100 M, Anton Paar). Silica rods were suspended in Milli-Q water at concentrations of 0.1-1 wt % and the suspension density was measured at 20 °C. The particle density was calculated using the formula (Murphy R. P., Hong K. & Wagner N. J. (2016). *Langmuir*, 32(33), 8424–8435),

$$\frac{1}{\rho_s} = \left(\frac{1}{\rho_p} - \frac{1}{\rho_m}\right) c_p + \frac{1}{\rho_m}$$

where, ρ_m, ρ_p and ρ_s are the densities of the solvent, particle and the suspension, respectively, and c_p is the particle mass fraction. The density of the rods was found ρ_p = 1.98 g/cm^3 (Figure S2).

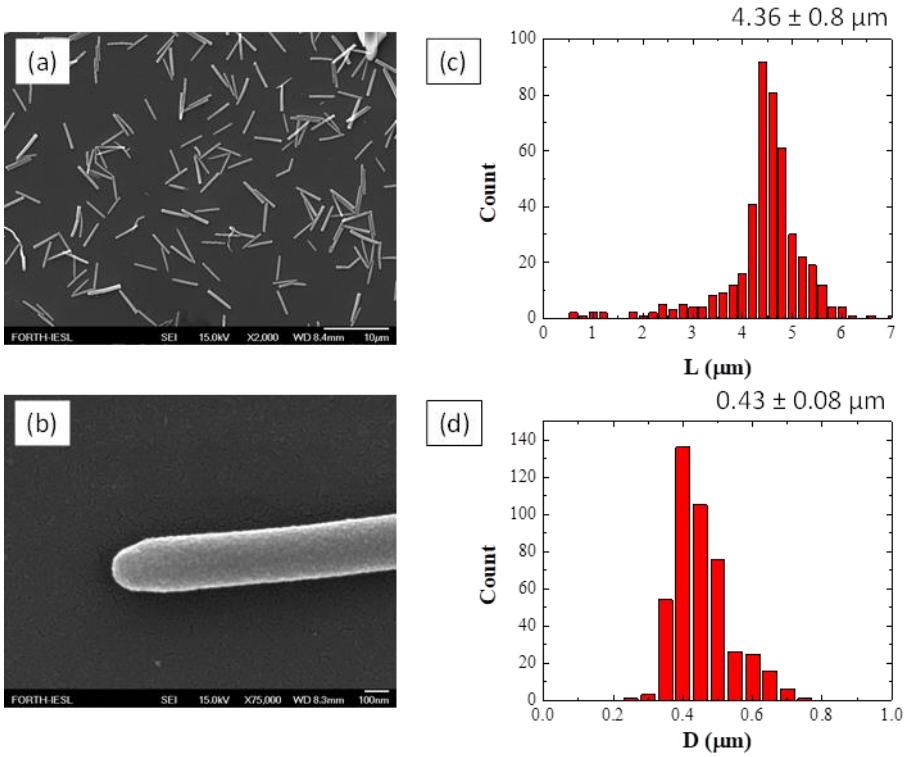

Figure S1 Scanning electron micrographs of silica rods (a, b) and distribution of length (c) and diameter (d) of rods obtained by image analysis.

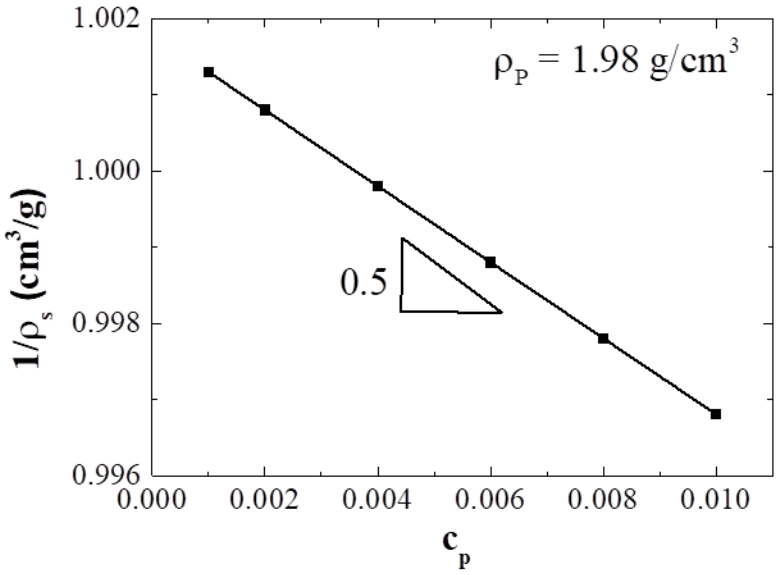

Figure S2 Silica rod mass fraction plotted against the inverse of suspension density. The particle density was obtained by a linear fit of the data.

2. Ageing after rejuvenation

We investigated the effects of shear cessation on the rod gel structure by measuring the linear viscoelastic response as well as microstructural changes using the rheo-confocal setup immediately after high shear rejuvenation. Three dimensional confocal micrographs were captured for a non-rejuvenated sample immediately after loading and at 60 sec intervals after cessation of shear until 2000 sec (= $600\tau_R$). The percentage of voids was measured in the captured confocal micrographs by first binarizing the image and then counting the number of pixels with the particles (Figure S 3).

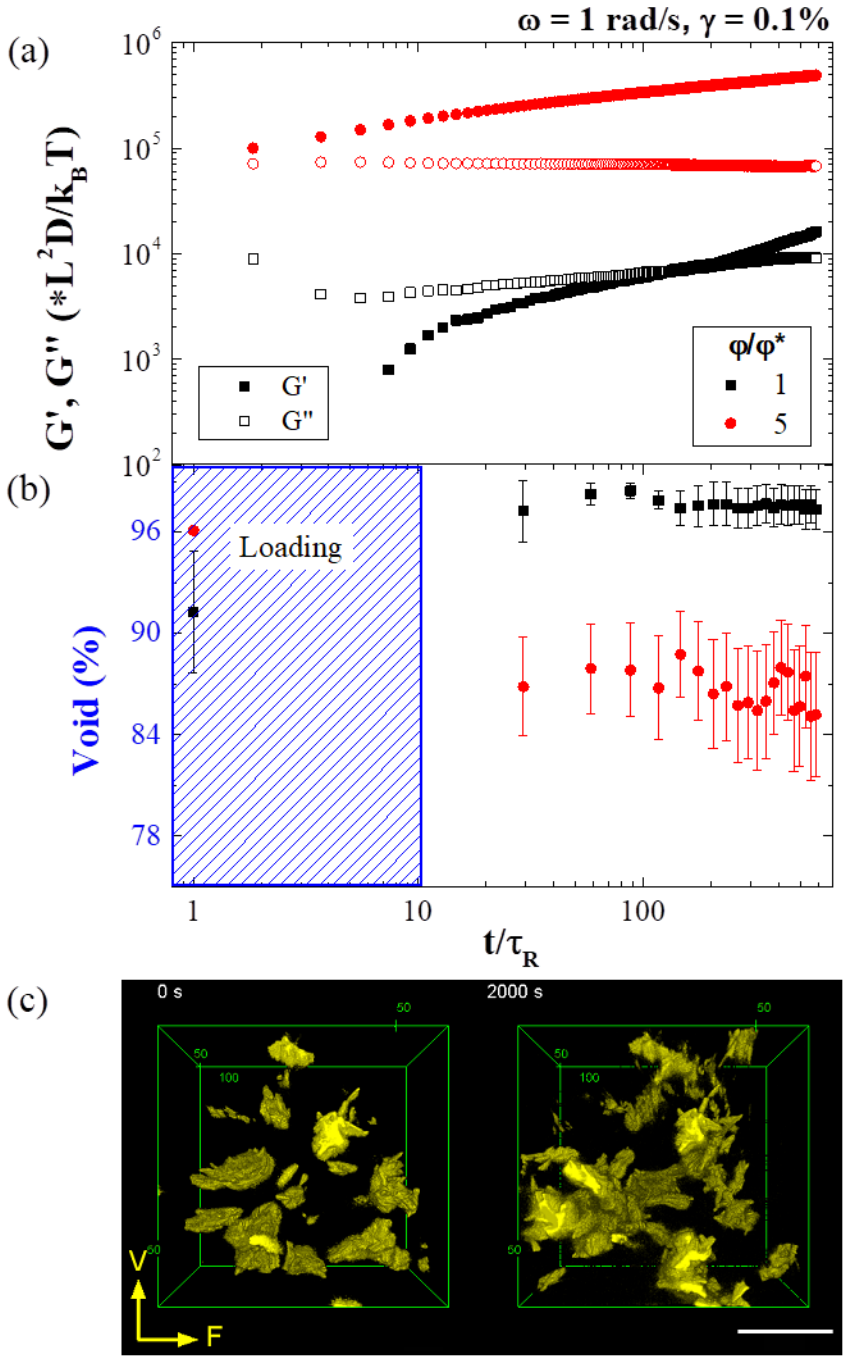

Figure S 3 (a) Time evolution of viscoelastic moduli of rod gels at 1 rad/s for two volume fractions ($\varphi/\varphi^* = 1$ and 5) and (b) time evolution of the percentage of voids in the suspension microstructure obtained from the confocal micrographs. (c) 3D confocal micrographs ($61\times61\times30$ μm^3) for $\varphi/\varphi^* = 1$ captured at t = 0 sec and t = 2000 sec after shear cessation. Scale bar: 20 μm.

3. Yielding under oscillatory shear

We captured the microstructure of the rod suspension ($\varphi/\varphi^* = 1$) while undergoing large amplitude oscillatory shear (LAOS) flow at an imposed strain of 200 % (Figure S 4). It was difficult to visually differentiate between structural changes at lower strains and hence a large strain of 200 % was chosen. The microstructure clearly shows a reversible bending and twisting process that is responsible for the yielding of the rod gels formed by screening the Coulomb interactions between the rods. For further clarity on the yielding process please refer to the video file provided as supplementary information.

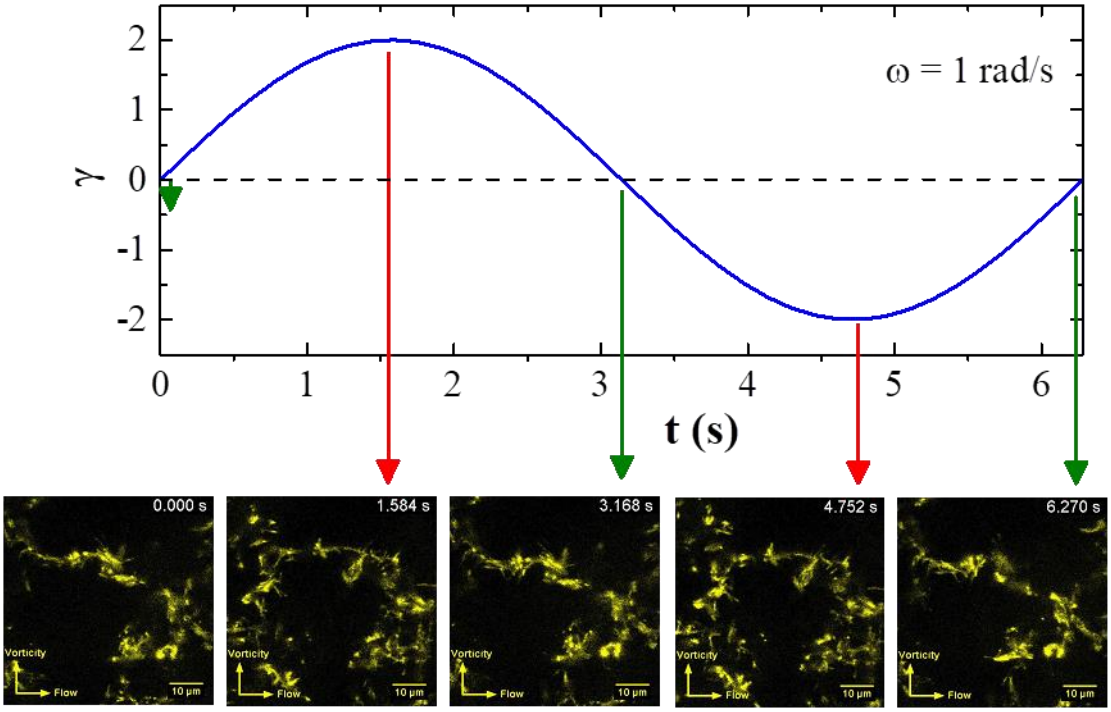

Figure S 4 Silica rod suspension ($\varphi/\varphi^* = 1$) microstructure captured using the rheo-confocal setup while undergoing large amplitude oscillatory shear (LAOS) flow at a strain of 200 %.

4. Volume fraction dependence of linear viscoelasticity

We compared the dependence of linear viscoelasticity (from DFS measurements) with the rod volume fraction (Figure S 5) and obtain a slope of 2 (approx.) which is lower than that reported previously with value around 4 (Shih et al., *Phy. Rev. A*, 1990). However, the yield or cross-over strain, γ_c reduced with increasing rod volume fraction showing that the gel structure becomes brittle with increasing particle concentration. This is qualitatively in agreement with studies on gels reported previously (Shih et al., *Phy. Rev. A*, 1990, Mohraz and Solomon, *J. Rheol.*, 2005).

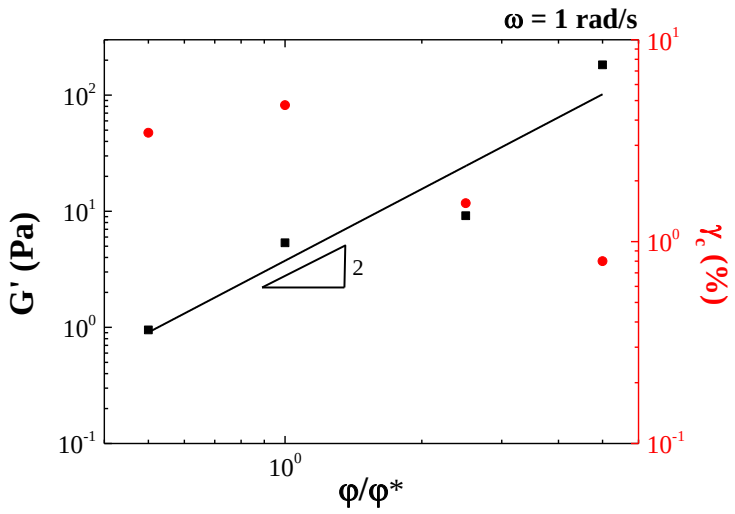

Figure S 5 Storage modulus (G') at 0.1% strain, 1 rad/s angular frequency and cross-over strain (γ_c) at different rod gel volume fractions.

5. Start-up shear of rod gels

We measured the stress response at $Pe_r = 1$ for different rod volume fractions of attractive rod suspensions (Figure S6). The transient stresses were related to structural heterogeneities, specifically to log – rolling particle rich flocs at low volume fractions ($\varphi/\varphi^* \leq 2.5$).

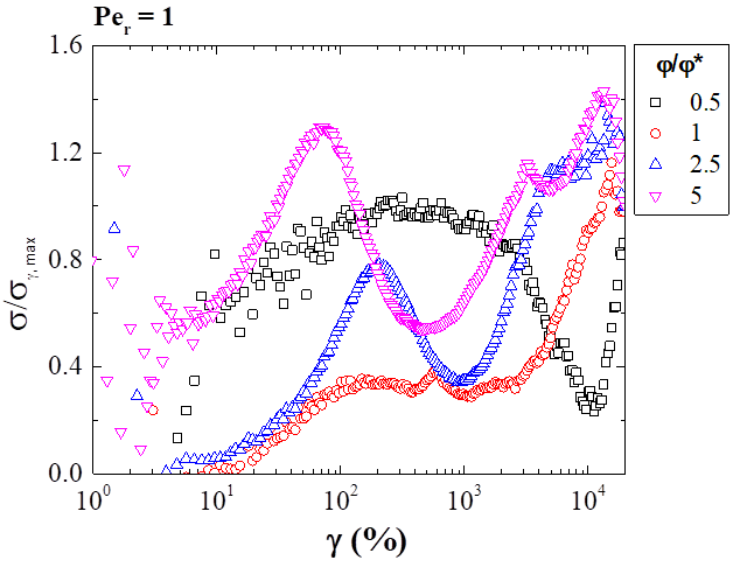

Figure S6 Transient stress response normalized by the stress at maximum imposed strain for rod suspensions at different volume fractions during start-up shear flow performed at $Pe_r = 1$.

6. Supplementary videos:

i) **Title: Ageing_Combined**

Demonstrates the formation of percolated gel structure after high shear rejuvenation using three dimensional confocal micrographs.

ii) **Title: flow curve_CP**
Using Type A imaging, we demonstrate formation of vorticity aligned flocs in a glass cone – plate geometry during descending shear rate sweep.

iii) **Title: 500 um gap_PP**
Shear banding phenomenon observed using Type A imaging in a glass parallel plate geometry at a gap of 500 μm.

iv) **Title: LAOS 200%_Phi star_Movie**
Two dimensional confocal micrographs captured for a rod gel suspension at volume fraction, $\varphi/\varphi^* = 1$ undergoing large amplitude oscillatory shear (200 %) flow using rheo-confocal setup.